

Analysis of damping-induced phase flips of plasmonic nanowire modes*

Andreas Hohenau¹, Primoz Kusar, Christian Gruber, and Joachim R. Krenn

Institute of Physics, Karl-Franzens-University, Universitätsplatz 5, 8010 Graz, Austria

¹Corresponding author: andreas.hohenau@uni-graz.at

Abstract

We launch surface plasmons from one end of a silver nanowire by asymmetric illumination with white light and use plasmon-to-light scattering at the nanowire ends to probe spectroscopically the plasmonic Fabry-Perot wire modes. The spectral positions of the maxima and minima in the scattered intensity from both nanowire ends are found to be either in phase or out-of phase, depending on the nanowire length and the spectral range. This behavior can be explained by a generalized Fabry-Perot model. The turnover-point between the two regimes is sensitive to the surface plasmon round trip losses and thus opens a new possibility for detecting changes of the optical absorption in the nanowire environment.

Surface plasmons (SP) are coherent oscillations of the electron density at the interface of a metal to a dielectric. In analogy to light in dielectric fibers, SPs in the optical spectral range are guided by noble metal nanowires [1,2]. In contrast to dielectric structures plasmonic nanowires show however no cutoff behavior as the SP wavelength scales with the nanowire cross-section dimension [3]. Due to the confined SP electromagnetic fields, nanowires couple efficiently to nearby photon emitters [4–6], making them promising building blocks in quantum optics. The coupling of light to nanowire SPs (and vice versa) and the SP end-face reflection is governed by the geometry of the wire end faces [7] and gives rise to SP Fabry-Perot (FP) modes, as has been observed by optical dark-field micro-spectroscopy [8,9]. Here, we use this technique to reveal a distinct phase-flip in the resonance positions measured from both nanowire ends, whose spectral position is sensitive to the guided SP mode round-trip losses.

Silver nanowires were chemically synthesized by a seed-assisted reduction of AgNO_3 with ethylene glycol in the presence of poly(vinyl pyrrolidone) [10]. The resulting wires with cross-section dimensions around 100 nm and length up to a few tens of μm were spin cast in an ethanol solution on glass substrates. The substrates were optically immersed to a glass prism and illuminated with a slightly focused white light beam from a halogen lamp under total internal reflection. This excitation geometry allows a

*©2012 OSA. This article was published in Optics Letters **37**(4), 746 (2012) and is made available with the permission of OSA. The paper can be found at the following URL on the OSA website: www.opticsinfobase.org/ol/abstract.cfm?uri=ol-37-4-746. Systematic or multiple reproduction or distribution to multiple locations via electronic or other means is prohibited and is subject to penalties under law.

dark field detection, as the microscope objective (100x, numerical aperture 0.95) only collects light individually scattered from the *input* (I) and *distal* (D) nanowire ends (Fig. 1). The collected light is dispersed by a spectrophotometer and detected by a camera. For all experiments the excitation light is polarized in the plane of incidence which coincides with the long nanowire axis.

Fig. 2 depicts the experimentally recorded scattering spectra for two nanowires of 19 μm (a) and 5 μm (b) length. The intensities recorded from the distal wire ends $I_{s,D}$ show the typical periodic modulations attributed to SP-FP resonances [8]. For the 19 μm long nanowire the (weaker) intensity scattered from the input end ($I_{s,I}$) is in counter-phase to $I_{s,D}$ scattered at the distal end. This is generally expected in analogy to a FP-interferometer from the viewpoint of energy conservation. If the transmission (corresponding to $I_{s,D}$ in the nanowire case) is large, the reflection (corresponding to $I_{s,I}$ of the nanowire case) has to be small and vice versa [8]. However, for the 5 μm long nanowire, $I_{s,I}$ changes from being in-phase with $I_{s,D}$ at photon energies below ~ 1.55 eV to being in counter-phase above which deviates from the expectations for a FP-interferometer.

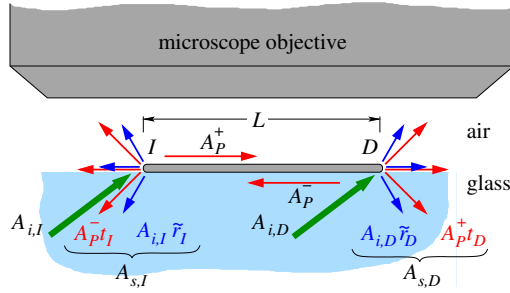


Figure 1: Sketch of a silver nanowire on glass substrate. The nanowire was illuminated from the glass substrate in total internal reflection geometry (thick, green arrows). The light scattered from the input (I) and distal (D) end of the wire is collected by a microscope objective and imaged on the input of a spectrograph. $A_{i,n}$ and $A_{s,n}$ are the amplitudes of the light incident and scattered from the input ($n = I$) or distal ($n = D$) end. A_P^+ and A_P^- are the amplitudes of the excited right and left propagating SP mode, respectively, and r and t are the reflection, transmission and scattering efficiencies as described in the text.

To gain a qualitative understanding of the observed behavior, we develop in the following a generalized FP model suitable for describing the scattering at the nanowire ends. In analogy to a FP-interferometer, the following (in general frequency dependent) coefficients are defined (Fig. 1):

- The direct scattering efficiency $\tilde{r}_n = A_{s,n}/A_{i,n}$ for the in-coupling ($n = I$) and distal ($n = D$) nanowire ends, where $A_{s,n}$ is the (complex valued) amplitude of the locally scattered light and $A_{i,n}$ is the amplitude of the excitation light at the respective nanowire end.
- The SP mode excitation efficiency $\tilde{t}_n = A_{P,t,n}/A_{i,n}$ at the nanowire ends, where

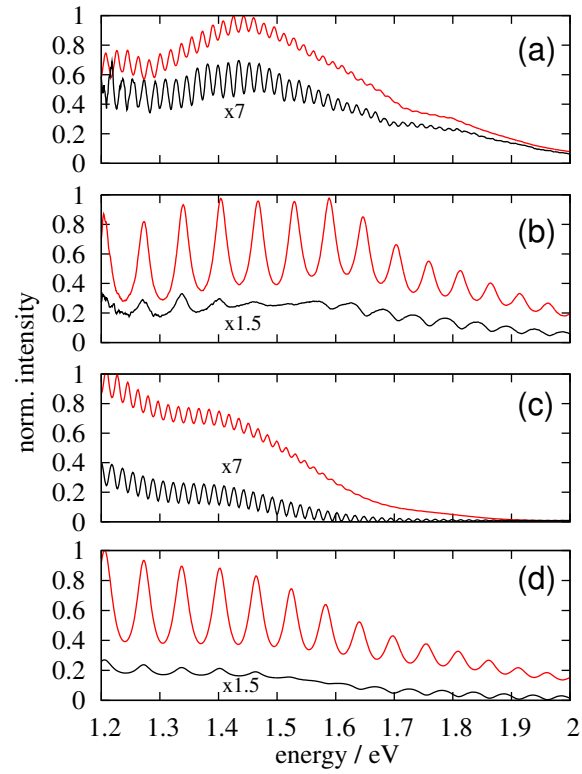


Figure 2: (a,b): Experimentally recorded scattering spectra of (a) a 19 μm and (b) a 5 μm long silver nanowire of the input (lower, black curves) and distal (upper, red curves) ends. (c,d): Theoretical scattering spectra calculated by a generalized FP model for (c) a 19 μm and (d) a 5 μm long nanowire (see text).

$A_{P,t,n}$ is the amplitude of the SP mode excited at end n .

- The SP mode reflection coefficient at the nanowire ends $r_n = A_{P,r,n}/A_{P,i,n}$, where $A_{P,r,n}$ and $A_{P,i,n}$ are the amplitudes of the reflected and incident SP at the nanowire end n , respectively.
- The SP scattering efficiency $t_n = A_{s,P,n}/A_{P,n}$, with $A_{s,P,n}$ being the amplitude of the light emitted from the nanowire ends due to scattering of the incident SP mode with amplitude $A_{P,n}$.

With A_P^+ and A_P^- denoting the amplitudes of the left- and right-propagating SP modes, one obtains:

$$\begin{aligned} A_{i,I}\tilde{t}_I + A_P^- r_I &= A_P^+ \\ A_{i,D}\tilde{t}_D + A_P^+ e^{ikL} r_D &= A_P^- e^{-ikL} \\ A_{s,D} &= A_P^+ e^{ikL} t_D + A_{i,D}\tilde{r}_D \\ A_{s,I} &= A_P^- t_I + A_{i,I}\tilde{r}_I \end{aligned} \quad (1)$$

This leads to

$$\begin{aligned} A_{s,I} &= A_{i,I}\tilde{r}_I + e^{ikL} \frac{A_{i,D}\tilde{t}_D t_I + A_{i,I} r_D t_I \tilde{t}_I e^{ikL}}{1 - r_I r_D e^{2ikL}} \\ A_{s,D} &= A_{i,D}\tilde{r}_D + e^{ikL} \frac{A_{i,I}\tilde{t}_I t_D + A_{i,D} r_I t_D \tilde{t}_D e^{2ikL}}{1 - r_I r_D e^{2ikL}} \end{aligned} \quad (2)$$

For the following, we make the simplification $r_I = r_D = r$, $t_I = t_D = t$ (justified for identical shapes of both nanowire ends) and the assumption that $\tilde{t}_D \simeq 0$ [8] and $\tilde{r}_D \simeq 0$. Already small deviations from this assumption cause alternating larger and smaller amplitudes of neighboring peaks in the scattering spectra of $I_{s,I}$ and/or $I_{s,D}$, which is not observed in Fig. 2. Consequently, the related intensities are

$$\begin{aligned} I_{s,D} &\propto |A_{s,D}|^2 \propto I_i \left| \frac{\tilde{t}_I t}{1 - r^2 e^{2ikL}} \right|^2 \text{ and} \\ I_{s,I} &\propto |A_{s,I}|^2 \propto I_i |\tilde{r}_I|^2 \left| \frac{1 - (r^2 - r t \tilde{t}_I / \tilde{r}_I) e^{2ikL}}{1 - r^2 e^{2ikL}} \right|^2 \end{aligned} \quad (3)$$

We note that for an actual experimental setup the light collection efficiency given by the numerical aperture of the detection optics and the scattering diagram of $I_{s,n}$ ($n = I, D$) can be included to the above equations as additional factors to \tilde{r}_n and t_n .

For comparison to the experimental results, we plot in Fig. 2(c,d) the scattering spectra as calculated by Eq. 3. The complex SP-mode dispersion relation was approximated by that for a 100 nm diameter Ag wire [3, 11] in a homogeneous dielectric environment. To roughly reproduce the experimentally observed spectral periodicity, we used 1.85 as effective dielectric constant. The resulting SP-mode propagation length was additionally multiplied by a factor of 1.7 to better resemble experimental values [12]. Further, the r and t coefficients are assumed purely real and frequency independent as $r = \sqrt{0.4}$ [12] and $t = \sqrt{1 - r^2}$ (energy conservation at the end-cap). \tilde{r}_I was set to $-0.04\tilde{t}_I$ ($-0.01\tilde{t}_I$) for the 5 μm (19 μm). The different but comparable small values of \tilde{r}_I were chosen for a better accordance with the experiment and might be indicative for different end cap geometries of the two wires. Despite the simplified assumption of frequency independent scattering and reflection coefficients (responsible

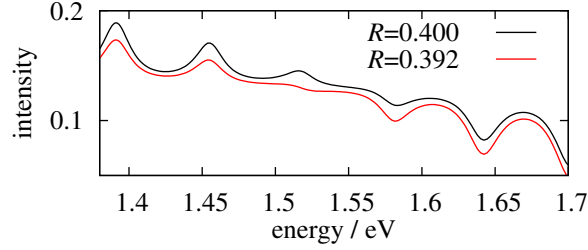


Figure 3: Calculated spectra of $I_{s,I}$ around the phase flip point for a 5 μm long nanowire. The SP end cap reflectivity is assumed as $R = |r|^2 = 0.4$ (upper, black curve) and $R = 0.392$ (lower, red curve). The resulting spectral shift of the phase flip point leads to a pronounced qualitative difference between the curves around this point.

for the discrepancies in “background”, modulation depth and the exact peak positions), good qualitative correspondence is observed between theory and experiment. This indicates, that the developed model indeed describes well the physics of the nanowire SP-FP-resonators.

As described above, particularly for the 5 μm long nanowire $I_{s,I}$ changes its qualitative behavior from being in-phase with $I_{s,D}$ at photon energies below ~ 1.8 eV to being in counter-phase above in both theory and experiment. This behavior is not expected from a FP-interferometer but is a peculiarity of the nanowire due to two reasons. First, the efficiency of direct scattering from the nanowire input end \tilde{r}_I (analog to the external reflectivity of a FP-interferometer) is much smaller than the SP reflection r , whereas in a usual FP-interferometer they are identical. Second, the excited SP modes suffer from propagation losses which are usually neglectable in a FP-interferometer. In combination of both, for a short nanowire (e.g. the 5 μm long wire) and in the red spectral range the SP round trip losses are small and the amplitude of the externally scattered light is neglectable against the amplitude of the light coupled out from the SP-FP mode. Thus the intensity of light scattered from both nanowire ends is dominated by the SP intensity only and maxima appear at the same spectral positions for both input and distal end. In contrast, for larger nanowire length (e.g. the 19 μm long wire) or in the blue spectral range of the spectrum for the 5 μm long wire, the amplitude of the SP-mode and thus that of the outcoupled light gets, due to ohmic losses, comparable or even smaller than the amplitude of the directly scattered light at the input end. If, as in a FP-interferometer, both are in counter-phase they interfere destructively. In the spectrum this leads to minima of the scattered light intensity at the input end at those spectral positions where the scattered light intensity of the distal end has maxima.

For the 5 μm long nanowire, both domains are within the spectral range, and the intensity profiles of $I_{s,I}$ changes its behavior from being in-phase with $I_{s,D}$ below ~ 1.55 eV to being in counter-phase above. The condition for this phase-flip can be derived from Eq. 3 as [13]

$$\tilde{r}_I = -\frac{t\tilde{t}_I}{r} \frac{\xi^2}{1 - \xi^2} \quad (4)$$

or

$$\xi^2 = \frac{\tilde{r}_I r}{\tilde{t}_I t + \tilde{r}_I r} \quad (5)$$

with $\xi = R|e^{2ikL}|$ as the SP-amplitude round trip losses. At this point one finds

$$I_{s,I} = I_i |\tilde{r}_I|^2 \frac{1}{\xi^2}, \quad (6)$$

and, for the ratio of the amplitude of the light scattered from the SP mode at the input end to that of the directly scattered light

$$\left| \frac{A_P^- r}{A_{i,I} \tilde{r}_I} \right| = 1 + \frac{1}{\xi}. \quad (7)$$

In contrast to the spacing of the maxima and minima in $I_{s,D}$ which depend on the round-trip phase, the spectral position of the phase-flip in $I_{s,I}$ depends on the SP round-trip losses only. For $\sim 2 - 7 \mu\text{m}$ long wires it could be used (in combination with the round trip losses determined from the spectra taken from the distal end [12]) to deduce the modulus of the direct scattering efficiency $|\tilde{r}_I|$ by Eq. 6, if the scattered intensity at the input end is measured quantitatively. Another application would be in nanowire sensor concepts as an information channel on the nanowire SP-mode propagation- and reflection losses to assess changes in the absorption of the nanowire environment or in the end cap reflectivity (for example caused by adsorbates or changes in the cap's geometry). Fig. 3 depicts the results of our calculations of $I_{s,I}$ around the phase-flip point, where the end-cap reflection r was lowered by 1% (red curve, the round-trip losses ξ are thus increased by 4%) leading to a pronounced qualitative change in $I_{s,I}$.

In conclusion, we demonstrated a phase change of the intensity scattered at the input end of a several μm long Ag nanowire compared to that scattered at the output end. By developing a generalized FP model adapted to the metal nanowire case, this feature can be explained by a combination of propagation losses of the excited SP modes and a relatively low efficiency for direct (i.e. without the involvement of the SP-FP mode) scattering of the exciting light at the input end. The spectral position of the phase-flip point is sensitive to the SP-mode round trip losses in the metal nanowire. It thus could be applied in nanowire sensors to assess changes in the SP losses in addition to the SP propagation constant probed by the spectral spacing of the transmission maxima.

Acknowledgement

Financial support from the European Union project ICT-FET 243421 ARTIST and from the Austrian Science Fund (FWF): P21235-N20 is acknowledged.

References

- [1] R. M. Dickson and L. A. Lyon, J. Phys. Chem. B **104**, 6095 (2000).

- [2] J. Dorfmueller, R. Vogelgesang, W. Khunsin, K. Rockstuhl, S. Etrich and K. Kern, Nano Lett. **10**, 3596 (2010).
- [3] J. Takahara, S. Yamagishi, H. Taki, A. Morimoto, and T. Kobayashi, Opt. Lett. **22**, 475 (1997).
- [4] D. E. Chang, A. S. Sørensen, P. R. Hemmer, and M. D. Lukin, Phys. Rev. Lett. **97**, 053002 (2006).
- [5] A. V. Akimov, A. Mukherjee, C. L. Yu, D. E. Chang, A. S. Zibrov, P. R. Hemmer, H. Park, and M. D. Lukin, Nature **450**, 402 (2007).
- [6] R. Kolesov, B. Grotz, G. Balasubramanian, R. J. Stöhr, A. A. L. Nicolet, P. R. Hemmer, F. Jelezko, and J. Wachtrup, Nature Phys. **5**, 470 (2009).
- [7] Z. Li, F. Hao, Y. Huang, Y. Fang, P. Nordlander, and H. Xu, Nano Lett. **9**, 4383 (2009).
- [8] H. Ditlbacher, A. Hohenau, D. Wagner, U. Kreibig, M. Rogers, F. Hofer, F. R. Aussenegg, and J. R. Krenn, Phys. Rev. Lett. **95**, 257403 (2005).
- [9] T. Shegai, V. D. Miljkovic, K. Bao, H. Xu, P. Nordlander, P. Johansson, and M. Käll, Nano Lett. **11**, 706 (2011).
- [10] D. Chen, X. Qiao, X. Qiu, J. Chen, and R. Jiang, J. Mater. Sci.: Mater. Electron. **22**, 6 (2011).
- [11] E. D. Palik, ed., *Handbook of optical constants of solids* (Academic Press, Inc., London, 1985).
- [12] P. Kusar, C. Gruber, A. Hohenau, and J. R. Krenn, Nano Letters **12**, 661 (2012).
- [13] Around this point $I_{s,i}$ has to be independent of k . By equating the coefficients of the cosine functions with identical periodicity in the denominator and numerator of $I_{s,i}$, one obtains after some algebra Eq. 4.